HARMONIC GENERATION AND LINEWIDTH NARROWING IN SEEDED FELS

L. Giannessi, ENEA Via E. Fermi 45, 00044, Frascati, Italy

Abstract

The process of harmonic generation in a seeded, single pass, Free Electron Laser, are studied in the time/frequency domain following the evolution of the harmonics within a self consistent time dependent model. The first and second order correlation functions of the fundamental and of the higher order harmonics fields are studied as a function of the input seed amplitude.

INTRODUCTION

Single pass Free Electron Lasers (FEL) operated in Self Amplified Spontaneous Emission (SASE) configuration are amplifiers of the natural shot noise of the driving electron beam. The spectral properties of the output radiation are the result of the amplification of the wide bandwidth noise arising from the stochastic distribution of the electron beam current, in the narrow bandwidth FEL amplifier. The properties of the output radiation, in terms of temporal coherence and intensity stability, have been extensively studied in literature [1][2][3] and reflect the stochastic nature of the electron beam shot noise. In a recent experiment at BNL[4] it has been shown that seeding a single pass FEL with an external laser allows to improve the spectral properties and the temporal stability of the laser source. In the same experiment it has been demonstrated that these properties are transferred to the higher order harmonics generated by the FEL. There is a widespread interest in this process, because emission on high order harmonics represents a significant resource to extend the wavelength tunability of an FEL and several recent proposals of FEL facilities rely on schemes based on seeding an harmonic generation[5]. The input seed, in order to be effective, must be characterized by enough intensity to overcome the intensity associated to the beam shot noise. The equivalent input intensity associated to a bunched beam is given by [6],

$$I_0 = \left|\left\langle \exp(\zeta_i)\right\rangle\right|^2 \frac{\rho P_e}{\Sigma_b} \tag{1}$$

where Σ_b is the electron beam cross section and $P_e = I_{peak} m_0 c^2 \gamma / e_0$ is the e-beam peak power. The parameter

$$\rho = \frac{1}{2\gamma}\left(\frac{\left[\lambda_u K\left(J_0(\xi) - J_1(\xi)\right)\right]^2}{4\pi\Sigma_b}\frac{I}{I_A}\right)^{\frac{1}{3}} \tag{2}$$

is the Pierce parameter, with $\xi = K^2 / \left[4\left(1 + K^2/2\right)\right]$, and $\zeta_i = (k + k_u) z_i - \omega t + \varphi_{0,i}$ are the electron phases in the ponderomotive potential associated to an undulator of period λ_u (with $k_u = 2\pi/\lambda_u$) and strength *K,* and to an optical field $E(z,t) = \widetilde{E}(z,t)\exp(i(\omega t - kz))$, being $\widetilde{E}(z,t)$ the slowly varying field component. In the specific case of randomly distributed electrons, the average $\left\langle \exp(\zeta_i)\right\rangle$ is the normalized sum of n_e independent phasors, i.e.,

$$\left|\left\langle \exp(\zeta_i)\right\rangle\right| = 1/\sqrt{n_e} \tag{3}$$

We estimate the number of interfering electrons n_e with the following naïve procedure. We define as

$$n_{1,e} = I_{peak}\lambda_0 / e_0 c \tag{4}$$

the number of electrons contained in a single resonant wavelength. Interference effects between electrons contained in contiguous wavelengths must be estimated. The field generated in a given longitudinal "slice" slips along the bunch and is amplified while the bunch travels along the undulator. This amplification must be considered in evaluating the interference between the fields emitted by electrons from different slices. The field evolution in presence of gain is given by [6],

$$\widetilde{E}(z) = \frac{E_0}{3}\left[e^{\left(\frac{i}{\sqrt{3}}+1\right)\frac{z}{2L_g}} + e^{\left(\frac{i}{\sqrt{3}}-1\right)\frac{z}{2L_g}} + e^{-i\frac{z}{\sqrt{3}L_g}}\right] \tag{5}$$

where $L_g = \lambda_u / \left(4\pi\sqrt{3}\rho\right)$ is the FEL gain length. We can use eq. (5) as a function of the longitudinal coordinate, to weight the electron number in each slice. Adding up the weighted number of electrons contained in all the slices, in a portion of the bunch of length $L\lambda_0/\lambda_u$, we get

$$n_e = n_{1,e}\int_0^L \left|E_0 / \widetilde{E}(z)\right| dz = f(L) I_{peak} L_g \lambda_0 / \lambda_u e_0 c \tag{6}$$

The dimensionless function $f(L)$ grows linearly with L for the first gain lengths, then converges rapidly to the constant ~ 4.3. Assuming $n_e \approx 4.3 I_{peak} L_g \lambda_0 / \lambda_u e_0 c$ as the total number of interfering electrons, we get from eq.(1)

$$I_0 \approx \lambda_u e_0 c / \left(4.3 I_{peak} L_g \lambda_0\right)\frac{\rho P_e}{\Sigma_b} \tag{7}$$

The equivalent input seed intensity I_0 can be estimated more accurately by considering the gain length corrections associated to diffraction/inhomogeneous effects [8][9]. In this paper we will study with a time dependent numerical model, the coherence properties of an FEL amplifier seeded with an input seed of amplitude varying across the "threshold" eq. (7).

TEST CASES AND NUMERICAL MODEL DESCRIPTION

The analysis of longitudinal coherence in a single pass FEL amplifier has been developed by implementing a 1D time dependent model of an FEL amplifier in PERSEO [10]. PERSEO is a library of FEL dedicated functions available in the Mathcad environment. The basic element of PERSEO is a FEL pendulum-like equation solver for the particle dynamics, coupled with the field equations in the slowly varying envelope approximation (SVEA). The integrator includes self consistently the higher order harmonics. Transverse effects, as inhomogeneous broadening due to emittances, are accounted for by introducing an equivalent energy spread. In order to include time dependency, both the slowly varying field distribution and the electron phase space distributions are sampled longitudinally. At each time step the longitudinal slippage of radiation over the electron beam is applied shifting the radiation parameters array over the electron parameter arrays by an interpolation procedure. The implementation is capable of simulating the FEL interaction process for any profile of the input field/e-beam current, satisfying the SVEA approximation. In the cases studied, a continuous current distribution/input seed distribution, with a periodic boundary condition in the simulation window, has been considered. This choice allowed to minimize the number of parameters affecting the results. In table 1 the main simulation parameters are shown.

Table 1: Main simulation parameters.

Case label	***A***	***B***	***C***
λ_0 (nm)	50	15	5
Undulator K (peak)	2.2	2.2	2.2
Energy (MeV)	500	900	1550
En. spread (MeV)	0.4	0.4	0.4
I_{peak}(A)	500	800	1500
N. emitt.(mm-mrad)	1	1	1
Σ_b (mm^2)	3.2×10^{-2}	1.8×10^{-2}	1.04×10^{-2}
Pierce parameter ρ	2.86×10^{-3}	2.26×10^{-3}	1.94×10^{-3}
I_0, eq.(1) (W/cm^2)	4.4×10^{4}	2.9×10^{5}	1.9×10^{6}
Sim. window (μm)	250	200	200
Sampl. period (μm)	0.625	0.5	0.5
Sim. bandwidth	4%	1.5%	0.52%

We have selected three configurations with the operating wavelength in the VUV. This choice is driven by the general interest in seeding FELs with very high order harmonics of the Ti-Sa laser, generated in gases[11]. These sources span the VUV region of the spectrum with a considerable level of peak power and constitute interesting candidates for seeding FEL amplifiers[5]. From the numerical representation point of view, at these wavelengths diffraction effects in the FEL dynamics are less severe. This mitigates the lack of accuracy due to the one dimensional FEL model implemented in PERSEO.

RESULTS

The statistics of radiation and its coherence properties are studied with the first and second order correlation functions. In the time domain, the first order classical correlation function is defined by [12]

$$g_1(\tau) = \frac{\left\langle \tilde{E}(t)\tilde{E}^*(t+\tau)\right\rangle}{\sqrt{\left\langle \left|\tilde{E}(t)\right|^2\right\rangle\left\langle \left|\tilde{E}(t+\tau)\right|^2\right\rangle}} \tag{8}$$

An estimation of the coherence length can be obtained by the relation [12]

$$z_c = c\int_{-\infty}^{+\infty}\left|g_1(\tau)\right|^2 d\tau \tag{9}$$

In the hypothesis of a SASE FEL operating in the exponential growth regime, the coherence length (9) is a monotonic growing function of the longitudinal coordinate z in the undulator, and reads [3],

$$z_c = \frac{1}{6}\frac{\lambda_0}{\rho}\sqrt{\frac{z}{2\pi L_g}} \tag{10}$$

In fig.1, the coherence length evaluated according to eq.(10) has been compared with the values calculated from the simulation data,

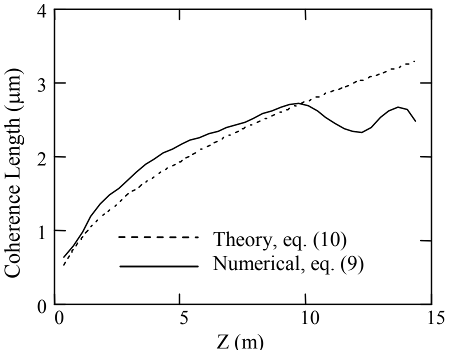

Fig. 1. Coherence length as given by eq. (10) (dashed line) and as calculated from the simulation data, according to eq.(9) (continuous line)

The plot in fig. 1 has been obtained simulating the configuration in column A of table 1, starting from the natural shot noise (no input seed). The beam energy spread has been set to zero in order to preserve the homogeneous conditions in which eq.(10) has been derived. The agreement is reasonable until saturation, which is occurring at z~10m, is reached.

In fig. 2 the growth of the laser intensity as a function of the longitudinal coordinate is shown. The parameters are those of tab.1, col. *A,* with an input seed represented by a perfectly uniform classical wave of intensity I_s=3.1x10^5 W/cm^2.

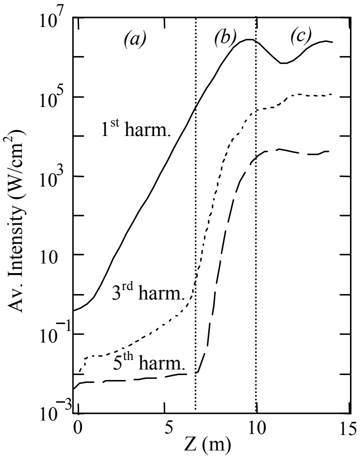

Fig. 2. Laser intensity vs. the longitudinal coordinate for the first three odd harmonics. The regions of exponential growth *(a)*, harmonics generation *(b)* and saturation *(c)* have been indicated in the figure.

In fig. 2 we can distinguish the region, labeled with *(b)*, where the growth of the third/fifth harmonic intensity is driven by the beam bunching due to the ponderomotive potential relevant to the first harmonic field.

The typical spectra for the third harmonic field, as calculated in regions *(a)* and *(b)* are shown in figs. 3.a,b respectively. In fig. 3.a the third harmonic field is not yet locked in phase to the bunching induced by the fundamental. The situation changes in fig. 3.b, where the phase of the third harmonic field is determined by the bunching on the fundamental and the coherence properties of the seed are transferred to the third harmonic. A similar behaviour is observed for the fifth harmonic.

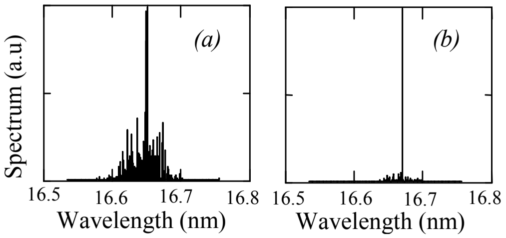

Fig.3. Third harmonic spectrum in the region *(a)* (at z~4.7m) and in the region *(b)* (at z~7.2m). The relative r.m.s. linewidth is ~0.174 % in *(a)* and ~0.076 % in *(b).*

In fig.4 it is shown the behaviour of the maximum coherence length reached along the undulator, as a function of the input seed intensity. The parameters are those of table 1, column *A*. At 500μm the coherence length saturates because of the limited extension of the simulation window (250μm). The value of the intensity calculated according to eq.(1) is shown as a vertical dashed line. In figs. 5 and 6 are shown the equivalent plots obtained with the parameters listed in columns *B* and *C* of table 1 respectively.

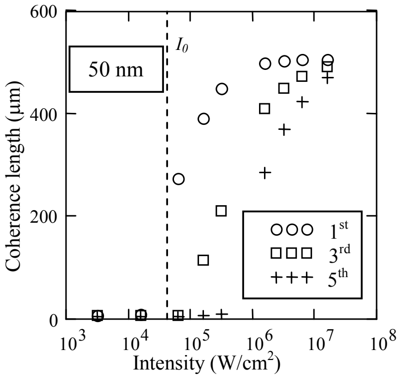

Fig. 4. Maximum coherence length reached along the undulator, as a function of the input seed intensity in the test case *A*. The dashed line indicates the threshold intensity I_0 evaluated according to eq. (7).

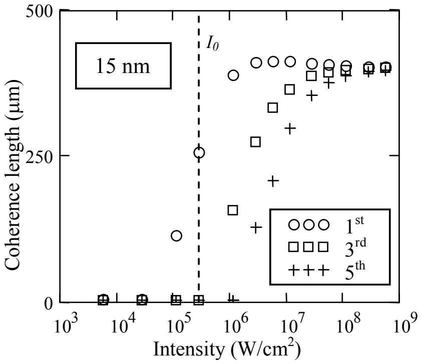

Fig. 5. As in fig.4 with the parameters of tab.1, col. *B*.

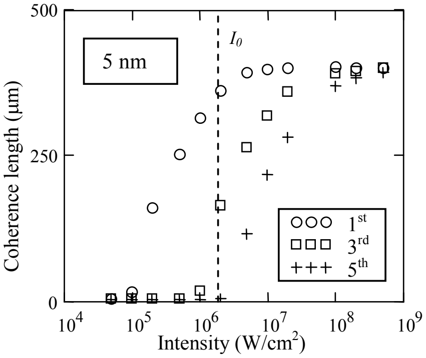

Fig. 6. As in fig.4 with the parameters of tab.1, col.*C*

As expected the power level required to ensure coherence on the higher order harmonics grows with the harmonic order. Comparing figs. 4, 5 and 6 it appears that the equivalent seed I_0 obtained according to eq.(7), slightly overestimates the intensity required to establish coherence on the fundamental harmonic, as the wavelength decreases (parameters of col. C, fig.6). It must be stressed that the intensity of eq.(1) still matches quite well the intensity that can be obtained by extrapolating the laser intensity at z=0 from the simulation data.

The intensity fluctuations have been studied calculating the second order correlation function $g_2(\tau)$ [12]:

$$g_2(\tau)=\frac{\left\langle \left|\tilde{E}(t)\right|^2 \left|\tilde{E}(t+\tau)\right|^2 \right\rangle}{\left\langle \left|\tilde{E}(t)\right|^2 \right\rangle \left\langle \left|\tilde{E}(t+\tau)\right|^2 \right\rangle} \qquad (11)$$

as a function of the longitudinal coordinate along the undulator. From the definition (11), and assuming $I(t) \propto \left|\tilde{E}(t)\right|^2$, it follows that

$$\sqrt{g_2(0)-1}=\left[I/\langle I\rangle\right]_{RMS} \qquad (12)$$

In figs.7, 8 and 9 it is shown the minimum along the undulator of the r.m.s. intensity (12), as a function of the seed intensity, in the cases *A*, *B* and *C* respectively. The averages in (12) are taken over the temporal extension of simulation window.

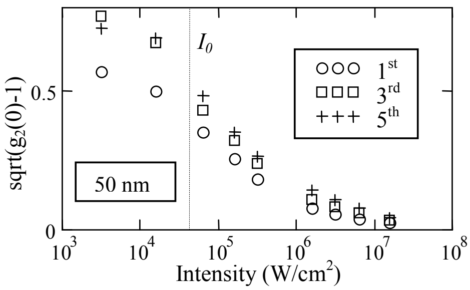

Fig. 7. Standard deviation of the intensity fluctuations vs. the seed intensity with the parameters of tab.1, col. *A*

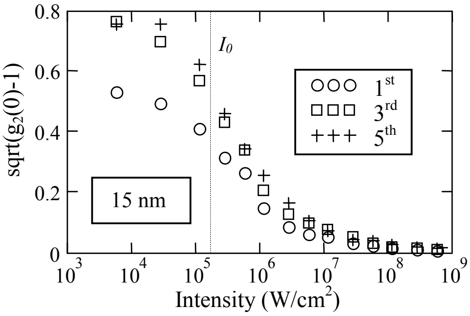

Fig. 8 As in fig. 7, with the parameters of tab.1, col. *B*

In a SASE FEL in the exponential growth regime, we have $\sqrt{g_2(0)-1}=1$ [3]. As expected the effect of the seed is that of suppressing the intensity fluctuations but this transition is smoother than the one observed in establishing the temporal coherence (figs. 4,5 and 6).

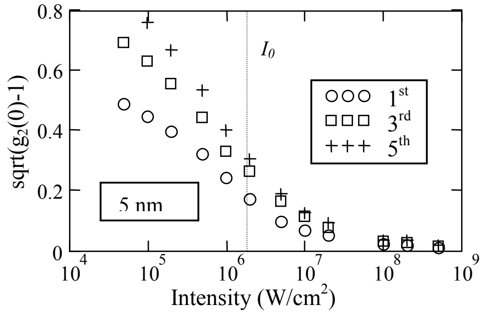

Fig. 9. As in figs. 7,8 with the parameters of tab.1, col. *C*

Fluctuations of the higher order harmonics are larger than fluctuations on the fundamental. The amplitude of the seed required for suppressing the fluctuations exceeds by orders of magnitude the intensity provided by eq.(7).

CONCLUSIONS

We have analysed the coherence properties of a seeded FEL amplifier as a function of the seed amplitude. The equivalent intensity associated to the beam shot noise, eq.(7), has been compared to the transition to coherence induced by the presence of a seed. The results obtained so far constitute a preliminary analysis which gives an indication about the power requirements of the input seed, in order to be effective in improving the coherence properties of a single pass FEL.

REFERENCES

[1] R. Bonifacio, L. De Salvo, P. Pierini, N. Piovella, C. Pellegrini, Phys. Rev. Lett. 73 (1994) 70 and references therein.
[2] P. Pierini, W. M. Fawley, Nucl. Instrum. & Meth. A 375 (1996) 332-335
[3] E.L. Saldin, E.A. Schneidmiller, M.V. Yurkov, Optics Communications 148, (1998) 383–403
[4] L. H. Yu et al., Phys. Rev. Lett. 91 (2003) 74801
[5] Workshop on the Physics of Seeded Free Electron Lasers, 17-19 June 2004, MIT campus, Cambridge, MA http://mitbates.mit.edu/xfel/conference.htm
[6] G. Dattoli, P.L. Ottavini, Journal of Appl. Phys. 86 (1999) 5331
[7] See e.g. G. Dattoli, A. Renieri, A. Torre, Lectures on the Free Electon Laser Theory, World Scientific ed. (1993) p. 493
[8] M. Xie, in *Proceedings of the Particle Accelerator Conference, Dallas, TX, 1995* (IEEE, Piscataway, NJ, 1996), p. 183. Sect. A **483**, 101 (2002).
[9] G. Dattoli, L. Giannessi, P.L. Ottaviani, C. Ronsivalle, Journal of Appl. Phys. 95 (2004) 3206
[10] http://www.enea.perseo.it
[11] P. Salières et al., Science **292** (2001) 902
[12] See e.g. R. Loudon, Quantum Theory of Light, Oxford Univ. Press (2000), chapter 3.